

Interaction of electrons in a one dimensional system with a magnetic texture

(Undergraduate thesis)

Student: Seremetas Konstantinos
Supervisor: Prof. Xenophon Zotos
Academic year: 2023/2024

University of Crete
Department of Physics



Contents

• Abstract	3
• Introduction	3
- Domain walls.....	3
- Landauer-Buttiker formalism and the S matrix method.....	6
- Density of states and T matrix.....	8
• Methodology	11
• Results	14
- Transmission and reflection for magnetic textures with constant angular configuration.....	14
- Transmission and reflection for the $J \gg D$ and $D \sim J$ domain walls.....	16
- Conductance and density of states for the $J \gg D$ domain wall.....	18
- Conductance and density of states for the $J \sim D$ domain wall.....	21
• Discussion	23
• References	23

Abstract

In this project we calculated the conductance and density of states of a one dimensional electronic system in interaction with a Bloch type domain wall in magnetic materials. We approached the problem by a double exchange (s-d) Hamiltonian and making use of the transfer matrix method, we found by inversion the corresponding S matrix. From the elements of the S matrix it is then easy for us to calculate the conductance and the density of states of the system. We dedicate the last part of the report visualizing and commenting our results. This project is part of a bigger effort to understand how the electron-domain wall interaction can affect the spatial configuration of the domain walls.

Introduction

Domain walls

Domain walls are specific areas of magnetic materials that connect its magnetic domains. The magnetic domains consist of atoms whose magnetic moments are aligned and make this specific area of the material magnetized. They exist in ferromagnetic materials when the temperature is below the Curie limit and they are responsible for their permanent magnetic properties. These areas interact with the magnetic moments of the conducting electrons in a constant way and do not appear to have any special effect. Interesting results occur however when we try to examine the interaction of the electrons with the domain walls of the material. The determinant configuration of the spin wavefunction of the electrons plays a role in the way they travel through different types of domain walls. The study of this interaction gives us information about the thermodynamic and electronic properties of the material.

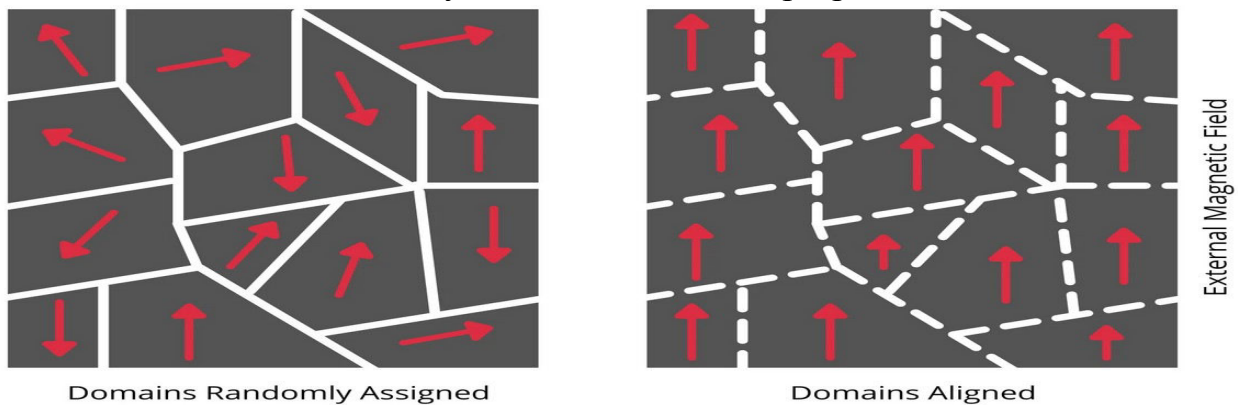


Figure 1: Magnetic domains in a magnetic material

There are two main types of domain walls, the Bloch type and the Néel type. The Bloch type domain walls appear mostly in bulk materials and consist of a spin

rotation parallel to the wall plane. Its length is defined by the value of $\sqrt{\frac{J}{D}}$ where J is the exchange energy and D is the anisotropy constant. When the film thickness becomes smaller than the domain wall the Bloch wall induces surface charges by its stray field and the Néel wall becomes more favorable. This type of domain wall consists of a spin rotation parallel to the film plane and its width is mainly defined by the value of $\sqrt{\frac{J}{K_d}}$ where K_d is the demagnetizing energy. Besides these two, there are also other types of domain walls such as the cross-tie wall which is a mixture of the Néel and Bloch domain walls. The following image gives us a visualization of what was discussed. This project is based on the study of the Bloch type domain walls.

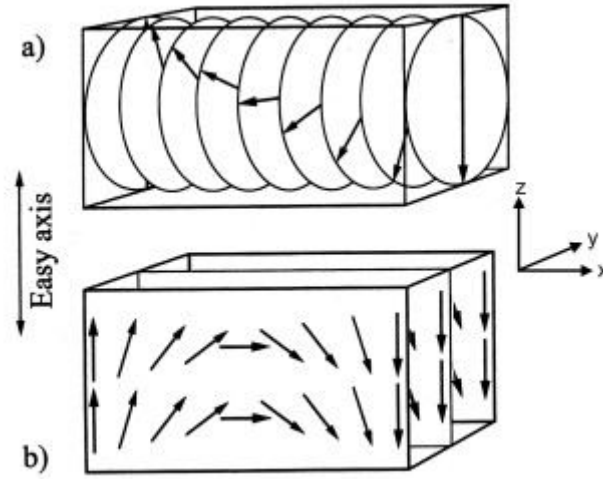


Figure 2: Visualization of the (a) Bloch domain walls and (b) Néel domain walls

The Hamiltonian of the regular ferromagnetic chain is:

$$H_{HA} = -2J S^2 \sum_{n=-\infty}^{+\infty} \vec{u}_n \vec{u}_{n+1} - D S^2 \sum_{n=-\infty}^{+\infty} u_{n,z}^2$$

The first term describes the exchange energy (assuming only the first neighbor interaction) while the second term is the anisotropy term.

For uniaxial anisotropy (the z axis is the easy axis) $D > 0$. The energy of the chain is:

$$E = -2J S^2 \sum_{n=-\infty}^{+\infty} \cos(\theta_n - \theta_{n+1}) + D S^2 \sum_{n=-\infty}^{+\infty} \sin^2(\theta_n) \quad (1)$$

where θ_n is the angle between the n spin vector and the z axis.

The energy of the domain wall is calculated by subtracting from (1) the energy of the chain without defects,

$$\frac{\Delta E}{2JS^2} = \sum_{n=-\infty}^{+\infty} (1 - \cos(\theta_n - \theta_{n+1})) + \frac{D}{2J} \sum_{n=-\infty}^{+\infty} \sin^2(\theta_n)$$

Minimizing the energy with respect to the spin angles gives us the spin configuration of the minimum energy state,

$$\frac{\partial \Delta E}{\partial \theta_n} = 0 \Rightarrow \sin(\bar{\theta}_n - \theta_{n+1}^-) + \sin(\bar{\theta}_n - \theta_{n-1}^-) + \frac{D}{2J} \sin(2\bar{\theta}_n) = 0 \quad (2)$$

The resulting angle configuration depends on the competition between J and D (in other words the D/J ratio). There are two cases: $D \gg J$ (narrower domain wall) and $D \ll J$ (broader domain wall). We choose the boundary conditions of the ferromagnetic chain to be $\bar{\theta}_i = 180^\circ$ and $\bar{\theta}_f = 0^\circ$. For the case where $D \gg J$ the spin angles are relatively small which allows us to linearize equation (2):

$$2\left(1 + \frac{D}{2J}\right)\bar{\theta}_n = \theta_{n-1}^- + \theta_{n+1}^-$$

Which gives us the following domain wall profile for $n > 0$:

$$\bar{\theta}_n = \theta_0 e^{-n\psi}$$

where

$$\cosh(\psi) = \left(\frac{D}{2J}\right) + 1$$

Close to the critical value $D/J = 4/3$ (for $D/J > 4/3$ it is easy to show that the domain wall has the length of a unit cell):

$$\bar{\theta}_0 = \sqrt{5(3 - e^\psi)}/2$$

For the case where $J \gg D$ we follow a similar procedure (we assume the spin angle as a continuous function of n). The result is the following:

$$\tan\left(\frac{\bar{\theta}}{2}\right) = e^{-n\sqrt{\frac{D}{J}}}$$

Landauer-Buttiker formalism and the S matrix method

The Landauer-Buttiker formalism is used in mesoscopic physics to describe the conductance of a crystal based on its scattering properties. A very effective way to study the scattering of a particle is using the S matrix method. The main idea behind the S matrix method is to calculate the outgoing (from the scatterer) part of the wavefunctions when we know the incoming part. Expanding these two wavefunctions into an orthonormal basis:

$$\Psi^{(\text{in})} = \sum_a A_a \Psi_a^{(\text{in})} \quad \Psi^{(\text{out})} = \sum_b B_b \Psi_b^{(\text{in})}$$

The S matrix helps us express the coefficients B_b when the coefficients A_a are known,

$$B_b = \sum_a S_{ba} A_a$$

Here S_{ba} are the elements of the S matrix.

$$\begin{bmatrix} \Psi_a \leftarrow \\ \Psi_b \rightarrow \end{bmatrix} = \begin{bmatrix} S_{11} & S_{12} \\ S_{21} & S_{22} \end{bmatrix} \begin{bmatrix} \Psi_a \rightarrow \\ \Psi_b \leftarrow \end{bmatrix}$$

Some of the interesting properties of the S matrix is that it is unitary:

$$S^\dagger S = S S^\dagger = I$$

Also:

$$\Psi(x, k) = \Psi^*(x, -k) \Rightarrow S^*(k) = S(-k)$$

In order to study a scattering problem between electrons and a potential barrier we consider the electrons to be non interacting and come from electron reservoirs. In order to study the current of electrons from the sample to the reservoirs and vice versa we use the second quantization formalism. It can be proved that the current operator for the channel α is:

$$\hat{I}_\alpha = \frac{e}{\hbar} \int \int dE dE' e^{it(E-E)/\hbar} [\hat{b}_\alpha^\dagger(E) \hat{b}_\alpha(E') - \hat{a}_\alpha^\dagger(E) \hat{a}_\alpha(E')]$$

Where the $\hat{a}_\alpha^\dagger(E)$ operator creates one electron in the incoming state with a wavefunction $\Psi_a^{(\text{in})}(E)/\sqrt{\hbar v_\alpha(E)}$ and the $\hat{b}_\alpha^\dagger(E)$ operator which creates the state

$\Psi_a^{(\text{out})}(E)/\sqrt{\hbar v_\alpha(E)}$. What we are actually interested is the measurable current $I_a = \langle \hat{I}_a \rangle$ which is calculated to be:

$$I_a = \frac{e}{\hbar} \int dE [f_a^{(\text{out})}(E) - f_a^{(\text{in})}(E)]$$

Here the functions $f_a^{(\text{in})}, f_a^{(\text{out})}$ are two distribution functions.

It is easy to show that $f_a^{(\text{in})}$ is equal to the Fermi distribution for the incoming electrons in the reservoir α ,

$$f_a(E) = \frac{1}{1 + e^{(E - E_f)/k_B T}}$$

We can find $f_a^{(\text{out})}(E)$ to be equal to:

$$f_a^{(\text{out})}(E) = \sum_{b=1}^N |S_{ab}|^2 f_b(E)$$

where N is the total number of reservoirs. This means that the current I_a is equal to:

$$I_a = \frac{e}{\hbar} \int dE \sum_{b=1}^N |S_{ab}|^2 [f_b(E) - f_a(E)]$$

If we apply a potential difference V_α the new value of the Fermi energy is

$$E'_f = E_f + e V_\alpha$$

If $|e V_\alpha| \ll k T_0$ we can use the following expansion for the Fermi function,

$$f_\alpha = f_0 - e V_\alpha \frac{\partial f_0}{\partial E} + O(V_\alpha^2)$$

This means that the current in the channel α will be

$$I_a = \frac{e^2}{\hbar} \int dE \sum_{b=1}^N |S_{ab}|^2 (-V_\alpha) \frac{\partial f_0}{\partial E}$$

And thus the conductance will be

$$G_a = \frac{-e^2}{\hbar} \int dE \sum_{b=1}^N |S_{ab}|^2 \frac{\partial f_0}{\partial E} \quad (3)$$

Density of states and T-matrix

We will now extract a theoretical formula which will make us able to evaluate the density of states (DOS) for a 1D system using the S matrix elements.

We begin by expanding the Green function of the system in the set of orthonormal eigenstates of the Hamiltonian of the system:

$$G(r, r', z) = \sum_n \frac{\varphi_n(r) \varphi_n^*(r')}{z - \lambda_n} \quad (4)$$

where λ_n is the eigenvalue of the eigenstate $\varphi_n(r)$.

We can write the retarded and the advanced Green function in the following form:

$$G(r, r', E) = \lim_{\varepsilon \rightarrow 0^+} G(r, r', E \pm i\varepsilon) \quad (5)$$

From equations (4) and (5) we get:

$$\lim_{\varepsilon \rightarrow 0^+} \int dr G(r, r', E \pm i\varepsilon) = \lim_{\varepsilon \rightarrow 0^+} \int dr \sum_n \frac{\varphi_n(r) \varphi_n^*(r')}{E - \lambda_n \pm i\varepsilon}$$

$$\lim_{\varepsilon \rightarrow 0^+} \int dr G(r, r', E \pm i\varepsilon) = \lim_{\varepsilon \rightarrow 0^+} \sum_n \frac{1}{E - \lambda_n \pm i\varepsilon}$$

$$\lim_{\varepsilon \rightarrow 0^+} \int dr G(r, r', E \pm i\varepsilon) = \pm i\pi \sum_n \delta(E - \lambda_n)$$

Consequently:

$$\rho(E) = \sum_n \delta(E - \lambda_n) = \pm \frac{1}{\pi} \lim_{\varepsilon \rightarrow 0^+} \Im \left(\int dr' G(r, r', E \pm i\varepsilon) \right)$$

Considering the retarded Green function we get:

$$\rho(E) = -\Im \frac{1}{\pi} \int dr G(r, r', E)$$

Setting $r=r'$

$$\rho(E) = -\frac{1}{\pi} \Im \int dr G(r, r, E)$$

$$\rho(E) = -\frac{1}{\pi} \Im \text{Tr} G(E) \quad (6)$$

This is the retarded Green function and $\rho(E)$ is the local density of states. Corresponding the fact that the Hamiltonian is given by:

$$H(r, p) = H_0(r, p) + V(r)$$

The retarded Green function follows a Dyson type equation,

$$G(r, r', E) = G_0(r, r', E) + \int dr_1 \int dr_2 G_0(r, r_1, E) T(r_1, r_2, E) G_0(r_2, r', E) \quad (7)$$

Substituting (7) into (6) we get for the local density of states,

$$\rho(r, E) = -\frac{1}{\pi} \Im (\varphi_n, \hat{G}_0(E) \hat{T}(E) \hat{G}_0(E), \varphi_n)$$

where the operators in the inner product are the retarded free Green function and the transfer matrix. In order to find the total density of states we just have to integrate the local density of states over the spatial coordinates, in our case r.

$$D(E) = \int_0^\infty dr \rho(r, E)$$

$$D(E) = -\frac{1}{\pi} \Im \text{Tr} [\hat{G}_0(E) \hat{T}(E) \hat{G}_0(E)]$$

It can be proved that the last equation can be written as

$$D(E) = \frac{1}{2\pi i} \frac{\partial}{\partial E} \text{Tr} [\ln(\hat{S}(E))]$$

Where $\hat{S}(E)$ is the S matrix operator equal to

$$\hat{S}(E) = \hat{I} - 2\pi i \delta(E \hat{I} - \hat{H}_0) \hat{T}(E)$$

The equation above for the total density of states gives us the contribution of the scattering potential to the shift of the total density of states. Now we need to evaluate the trace of the operator $\ln \hat{S}$. In order to do this we will need to define the operators

$$\hat{X}(E) = 2\pi i \delta(E \hat{I} - \hat{H}_0) \hat{T}(E)$$

We will now need to evaluate the trace

$$\text{Tr} \ln \hat{S} = \text{Tr} \ln(\hat{I} - \hat{X})$$

For this reason we will use the formula

$$\begin{aligned} \ln(\hat{I} - \hat{A}) &= -\sum_{n=1}^{\infty} \hat{A}^n / n \\ \ln(\hat{S}) &= \ln(\hat{I} - \hat{X}) = -\sum_{n=1}^{\infty} \hat{X}^n / n \end{aligned}$$

Using this transformation it is easy to get to the equation that we will use

$$\begin{aligned} D(E) &= \frac{1}{2\pi i} \frac{d}{dE} \text{Tr}[\ln(S(E))] \\ D(E) &= \frac{1}{2\pi i} \text{Tr}\left[S^\dagger \frac{dS}{dE}\right] \\ D(E) &= \frac{1}{4\pi i} \text{Tr}\left[S^\dagger \frac{dS}{dE} - S \frac{dS^\dagger}{dE}\right] \end{aligned}$$

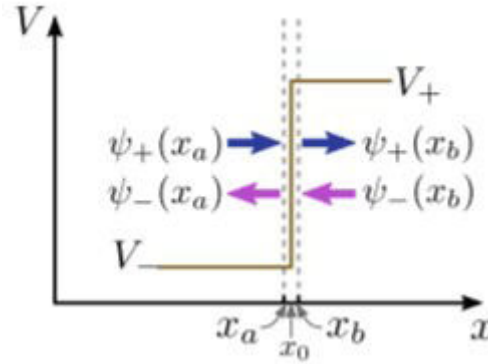
This is the final equation that we will use in our model in order to calculate the total density of states.

In order to find the S matrix we calculated the T matrix. The transfer matrix is similar to the scattering matrix but instead of correlating the incoming and the outgoing parts of the wavefunctions we use the left and the right from the potential parts of the wavefunction

$$\Psi^{(\text{left})} = \sum_a A_a \Psi_a^{(\text{left})} \quad \Psi^{(\text{right})} = \sum_b B_b \Psi_b^{(\text{right})}$$

$$A_a = \sum_b T_{ab} B_b$$

$$\begin{bmatrix} \Psi_a \rightarrow \\ \Psi_a \leftarrow \end{bmatrix} = \begin{bmatrix} T_{11} & T_{12} \\ T_{21} & T_{22} \end{bmatrix} \begin{bmatrix} \Psi_b \rightarrow \\ \Psi_b \leftarrow \end{bmatrix}$$



Methodology

We model our system with an s-d Hamiltonian, a method where we consider the electrons of the d orbital to be localized and produce a magnetic field that affects the behavior of the s orbital electrons which are assumed to be free conduction electrons. Our Hamiltonian is:

$$\frac{-\hbar^2}{2m} \frac{\partial^2}{\partial x^2} \Psi + (V(x) - E) \Psi = 0$$

where

$$V(x) = \vec{h}(x) \vec{\sigma}$$

For a random orientation of the magnetic field:

$$V(x) = \begin{bmatrix} h_z & h_x - i h_y \\ h_x + i h_y & -h_z \end{bmatrix} = \begin{bmatrix} h_z & h_- \\ h_+ & -h_z \end{bmatrix}$$

We also approach the wavefunction to be in the following form:

$$\psi = \begin{bmatrix} A_{\uparrow} \\ A_{\downarrow} \end{bmatrix} e^{iqx}$$

where the column vector represents the spin amplitudes of the electron. In the transfer matrix method we separate the potential in slices and suggest that it is constant in each one of the slices. Thus the wavefunction in each slice is that of a plane wave with a corresponding spin amplitude. We replace this form of Ψ in the Schrodinger equation above and we get:

$$\frac{\hbar^2 q^2}{2m} \begin{bmatrix} A_{\uparrow} \\ A_{\downarrow} \end{bmatrix} + \begin{bmatrix} h_z - E & h_- \\ h_+ & -h_z - E \end{bmatrix} \begin{bmatrix} A_{\uparrow} \\ A_{\downarrow} \end{bmatrix} = 0$$

We set

$$\frac{2m}{\hbar^2} = 1$$

which simplifies our eigenvalue problem. This relation also defines the units that are used. We thus have to solve

$$\begin{bmatrix} h_z - E + q^2 & h_- \\ h_+ & -h_z - E + q^2 \end{bmatrix} \begin{bmatrix} A_{\uparrow} \\ A_{\downarrow} \end{bmatrix} = 0$$

After the diagonalization we find the eigenvalues:

$$E_{1,2} = q^2 \pm h^2 \Rightarrow q = \pm \sqrt{E \mp h^2}$$

where h is the magnitude of the magnetic field.

The corresponding eigenvectors are:

$$\Psi_+ = \begin{bmatrix} +\cos(\varphi/2) \\ -\sin(\varphi/2) \end{bmatrix} \text{ and } \Psi_- = \begin{bmatrix} +\sin(\varphi/2) \\ +\cos(\varphi/2) \end{bmatrix}$$

where we have set

$$h_z = h \cos(\varphi), h_x = h \sin(\varphi)$$

The one dimensional spatial form of the grid is:

$$x_0 \text{ --- } x_1 \text{ --- } x_2 \text{ --- } \dots \text{ --- } x_N$$

where the x_i notation refers to the region $x_i < x < x_{i+1}$

Subsequently the wavefunction Ψ_i in the domain $x_i < x < x_{i+1}$ has the form:

$$\Psi_i(x) = A_i \begin{bmatrix} +\cos(\varphi/2) \\ -\sin(\varphi/2) \end{bmatrix} e^{+iq_i^+ x} + B_i \begin{bmatrix} +\cos(\varphi/2) \\ -\sin(\varphi/2) \end{bmatrix} e^{-iq_i^+ x} + C_i \begin{bmatrix} +\sin(\varphi/2) \\ +\cos(\varphi/2) \end{bmatrix} e^{+iq_i^- x} + D_i \begin{bmatrix} +\sin(\varphi/2) \\ +\cos(\varphi/2) \end{bmatrix} e^{-iq_i^- x}$$

We will now follow the connection procedure for the wavefunctions in each potential slice:

$$\Psi_i(x_{i+1}) = \Psi_{i+1}(x_{i+1}) \text{ and } \Psi_i'(x_{i+1}) = \Psi_{i+1}'(x_{i+1})$$

Setting

$$\Psi_i = \begin{bmatrix} A_i \\ B_i \\ C_i \\ D_i \end{bmatrix}$$

we can write:

$$u_i(x_{i+1}) \Psi_i = u_{i+1}(x_{i+1}) \Psi_{i+1}$$

where

$$u_i(x) = \begin{bmatrix} +\cos(\varphi_i/2)\exp(+i q_i^+ x) & +\cos(\varphi_i/2)\exp(-i q_i^+ x) & +\sin(\varphi_i/2)\exp(+i q_i^- x) & +\sin(\varphi_i/2)\exp(-i q_i^- x) \\ +i q_i^+ \cos(\varphi_i/2)\exp(+i q_i^+ x) & -i q_i^+ \cos(\varphi_i/2)\exp(-i q_i^+ x) & +i q_i^- \sin(\varphi_i/2)\exp(+i q_i^- x) & -i q_i^- \sin(\varphi_i/2)\exp(-i q_i^- x) \\ -\sin(\varphi_i/2)\exp(+i q_i^+ x) & -\sin(\varphi_i/2)\exp(-i q_i^+ x) & +\cos(\varphi_i/2)\exp(+i q_i^- x) & +\cos(\varphi_i/2)\exp(-i q_i^- x) \\ -i q_i^+ \sin(\varphi_i/2)\exp(+i q_i^+ x) & +i q_i^+ \sin(\varphi_i/2)\exp(-i q_i^+ x) & +i q_i^- \cos(\varphi_i/2)\exp(+i q_i^- x) & -i q_i^- \cos(\varphi_i/2)\exp(-i q_i^- x) \end{bmatrix}$$

From $u(x)$ the transfer matrix can be found in the following way:

$$\begin{aligned} u_i(x_{i+1}) \Psi_i &= u_{i+1}(x_{i+1}) \Psi_{i+1} \\ \Psi_i &= u_i^{-1}(x_{i+1}) u_{i+1}(x_{i+1}) \Psi_{i+1} \\ T_{i+1} &= u_i^{-1}(x_{i+1}) u_{i+1}(x_{i+1}) \\ \Psi_{N-1} &= T_N \Psi_N \end{aligned}$$

Consequently for N potential barriers the transfer matrix can be calculated as:

$$\begin{aligned} \Psi_0 &= T_1 T_2 T_3 \dots T_N \Psi_N \\ T &= T_1 T_2 T_3 \dots T_N \end{aligned}$$

Based on the calculations above we developed a code that gives us the transfer matrix for a specific domain wall. Having calculated the transfer matrix we can find the S matrix which is a 4x4 matrix.

The transfer matrix is correlating the amplitudes of the wavefunction in the region before and after the potential while the S matrix is correlating the amplitudes of the incoming with the outgoing waves.

$$\begin{bmatrix} A_1^{\uparrow \rightarrow} \\ B_1^{\uparrow \leftarrow} \\ C_1^{\downarrow \rightarrow} \\ D_1^{\downarrow \leftarrow} \end{bmatrix} = T \begin{bmatrix} A_N^{\uparrow \rightarrow} \\ B_N^{\uparrow \leftarrow} \\ C_N^{\downarrow \rightarrow} \\ D_N^{\downarrow \leftarrow} \end{bmatrix}$$

Considering a particle entering the potential region from the right in a spin up state we have the following equations:

$$\begin{aligned} 1 &= T_{11} A_N + T_{13} C_N \\ B_1 &= T_{21} A_N + T_{23} C_N \\ 0 &= T_{31} A_N + T_{33} C_N \\ D_1 &= T_{41} A_N + T_{43} C_N \end{aligned}$$

This means that:

$$A_N = S_{21\uparrow\uparrow}, C_N = S_{21\downarrow\uparrow}, B_1 = S_{11\uparrow\uparrow}, D_1 = S_{11\downarrow\uparrow}$$

We can repeat the same process setting $C_1=1$, $B_N=1$ and $D_N=1$ in order to calculate the rest of the S matrix elements.

After obtaining the S matrix elements it is easy for us to calculate the conductance and the density of states of the system using the formulas given in the introduction.

RESULTS

This code was used to calculate the previous electronic and thermodynamic quantities of the system and the results are given in this section. The x axis in the following diagrams refer to the electron energy.

First, we used this code to calculate the transmission and the reflection coefficients for a constant magnetic potential forming an angle with the z axis equal to zero. We consider the particle to be in the spin up state and moving towards the right.

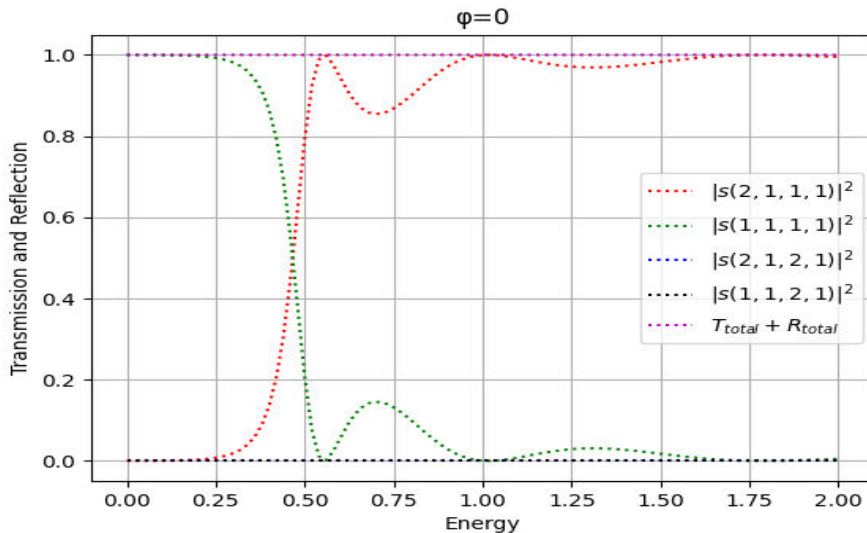


Figure 3: Scattering matrix elements for an electron in the spin up state entering a magnetic potential that is parallel to the z axis. The notation $s(a,b,c,d)$ corresponds to an electron that enters the potential ($\hbar=0.4$) at the point b and proceeds to get out at the point a. The initial spin state is d and the final and c. Etc if $a=b$ there is a reflection. Index 1 refers to the spin up state and index 2 refers to the spin down state. The $T_{\text{total}}+R_{\text{total}}$ is the sum of all the probabilities and appears as a check for our calculations.

The results are compatible with the known analytical results which get

$$r = \frac{(k^2 + q^2) \sin(qa) e^{-ika}}{(k^2 + q^2) \sin(qa) + 2iqk \cos(qa)} \quad \text{and} \quad t = \frac{2iqk e^{-ika}}{(k^2 + q^2) \sin(qa) + 2iqk \cos(qa)}$$

where $k^2=E$ and $q^2=E-V_0$.

Now let's see what happens when the magnetic field is not parallel to the z axis but forms an angle φ . The results appear to be rather complicated. We can explain them theoretically however if we consider the following operations. Supposing that the domain wall is on the zy plane, if we have a magnetic field that forms an angle φ with the z axis then we can calculate the new S matrix as

$$S' = R^{-1}(\varphi) S R(\varphi)$$

where S is the scattering matrix that corresponds to the case where $\varphi=0$ and

$$R(\theta) = \begin{bmatrix} \cos(\varphi) & \sin(\varphi) \\ -\sin(\varphi) & \cos(\varphi) \end{bmatrix}$$

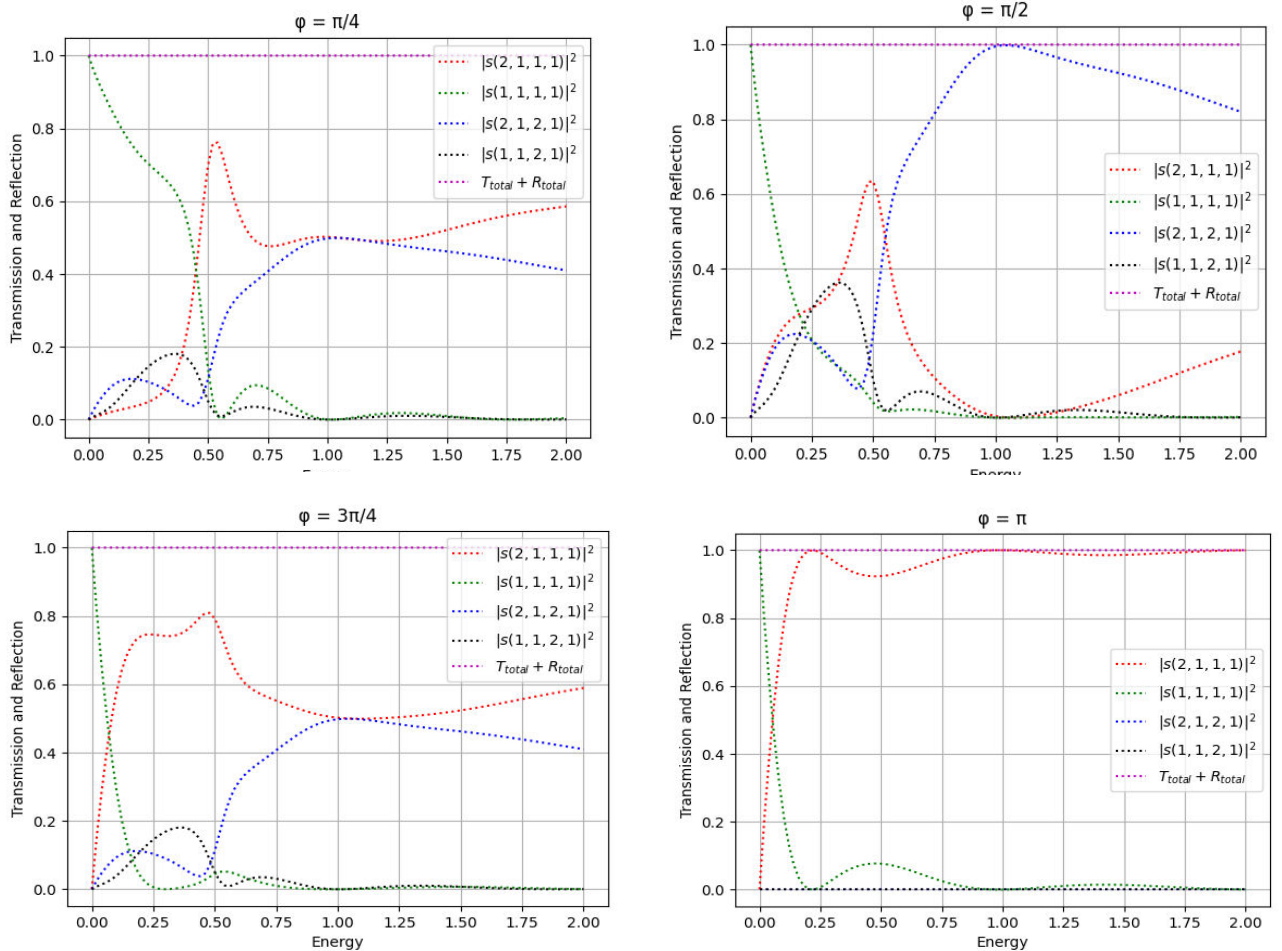


Figure 4: Electron in a spin up state enters a magnetic field whose direction forms and angle φ with the z axis. The value of the potential barrier is $h=0.4$.

We can observe that if the magnetic field does not form an angle with the z axis then the spin state of the electron after the scattering does not change. Additionally we can see that for high energies there is no reflection which is a result that agrees with our intuition. However we can also see some surprising results. For $\varphi=\pi/4$ there is an energy value $1 < E_0 < 1.25$ where the reflection probability is zero and there is an equal probability for the electron to transmit through the potential with spin up or spin down. The same thing and for the same energy value happens also in the case where $\varphi=3\pi/4$. In the case where $\varphi=\pi/2$ and for the same energy value the electron passes through the potential barrier as if it does not exist. This behavior has to do with coherence phenomena and the specific value of E where this happens depends on both the magnitude of the potential barrier and also its width.

Now let's use the code to graph the transmission and reflection behavior of one of the aforementioned domain walls:

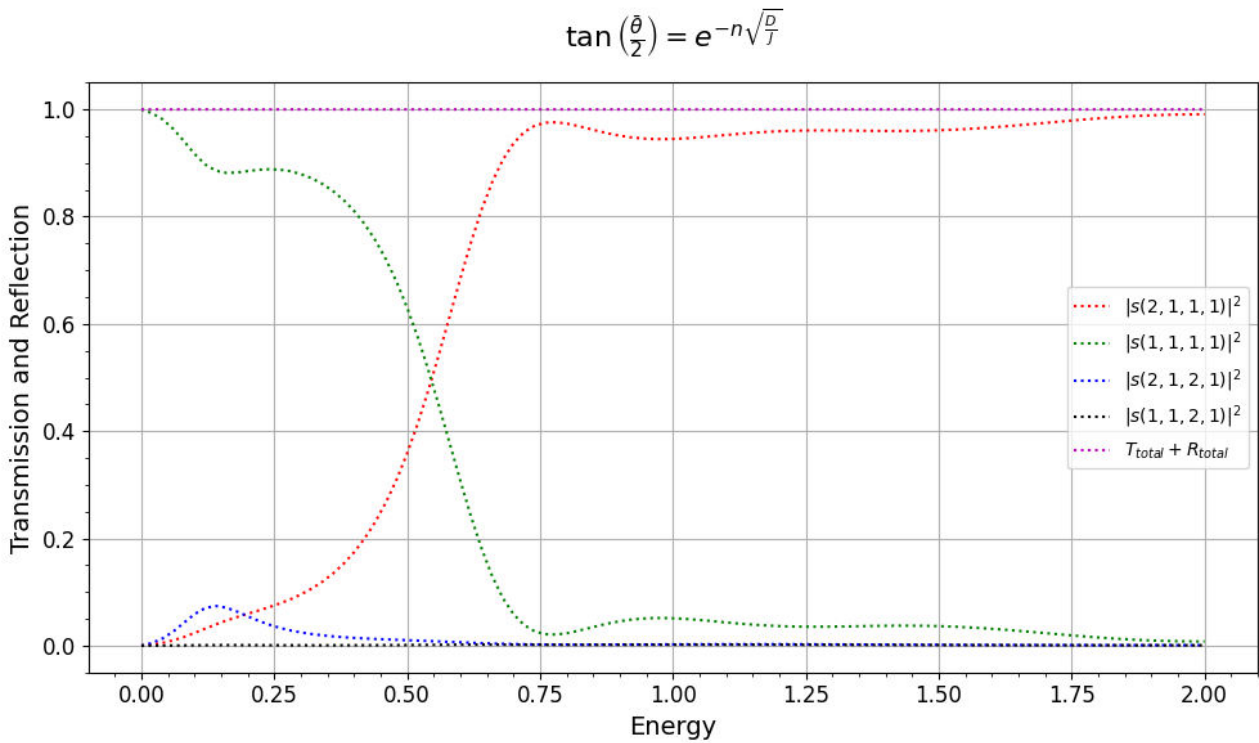


Figure 5: Transmission and reflection probabilities for an electron that enters in a spin up state the potential that is created by the domain wall that corresponds to the case where $J \gg D$. We used $h=0.4$ and $\delta=0.1$.

Now this is the first original result that occurred from our work and cannot be predicted analytically like the cases of the constant magnetic field that we showed before. In this case the electrons seem to keep their spin configuration almost intact since the transmission and reflection probabilities for the spin down state is almost zero for most of the energy values. We can see that there is a slight probability for the electron to transmit through the potential barrier and change its spin state. It is also

notable that there is zero probability for the electron to reflect from the potential barrier and change its spin.

It also as interesting to see how the transmission and reflection probabilities are configured for the other type of domain wall.

$$\bar{\theta}_n = \theta_0 \cdot e^{-n\psi}$$

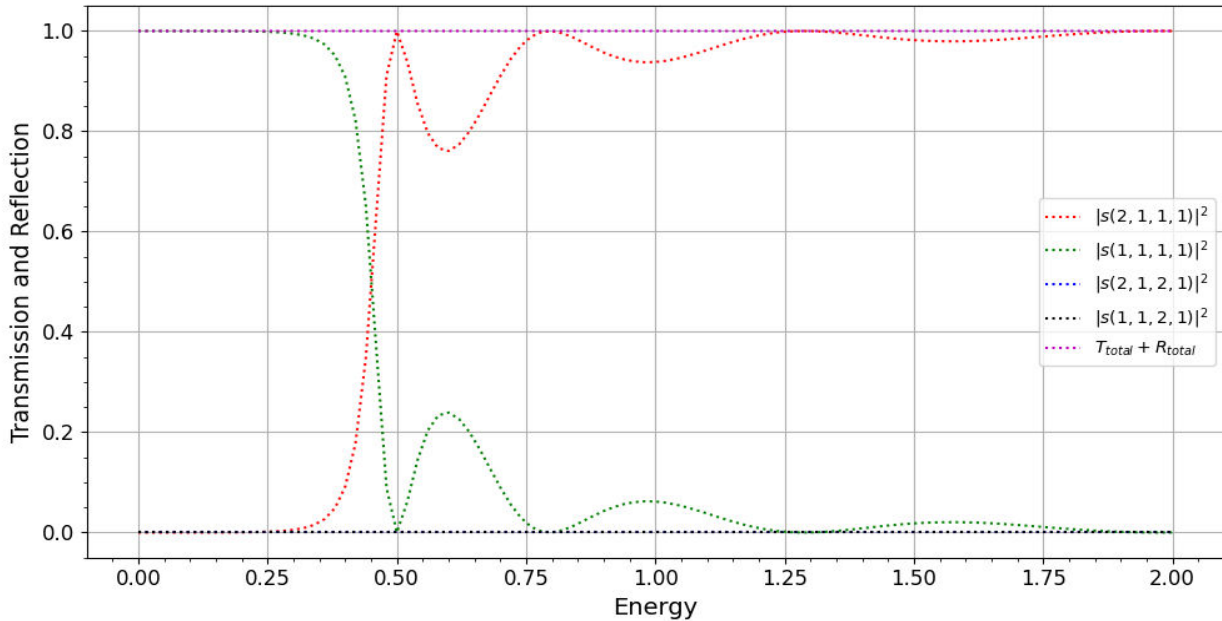


Figure 6: The transmission and reflection probabilities of an electron entering a magnetic potential in a spin up state that is created by the domain wall for the case $D \sim J$. We used $\hbar=0.4$ and $\delta=1.0$.

It is surprising to notice that although the direction of the magnetic field changes the electron has zero probability to change its spin state, either for transmission or for reflection.

Let's see now some more practical results. In the following pages we have visualized the behavior of some fundamental thermodynamic and electronic quantities of the magnetic material (conductance and density of states) in order to examine their behavior for different energy states of the electrons. In each occasion we study the behavior of these quantities for different values of the width of the domain wall $\delta=D/J$ (keeping in mind the approximation for the angular configuration of the domain wall is still valid), the chemical potential μ of the solid and beta $\beta=1/kT$.

For the domain wall $J \gg D$:

Let's start our investigation with the behavior of the conductance. The following diagram shows the variation of G for different values of $\beta=1/kT$. It is important to note that the conductance that appears in the following diagrams refers to the conductance per energy. The total conductance occurs when we integrate over all the energies.

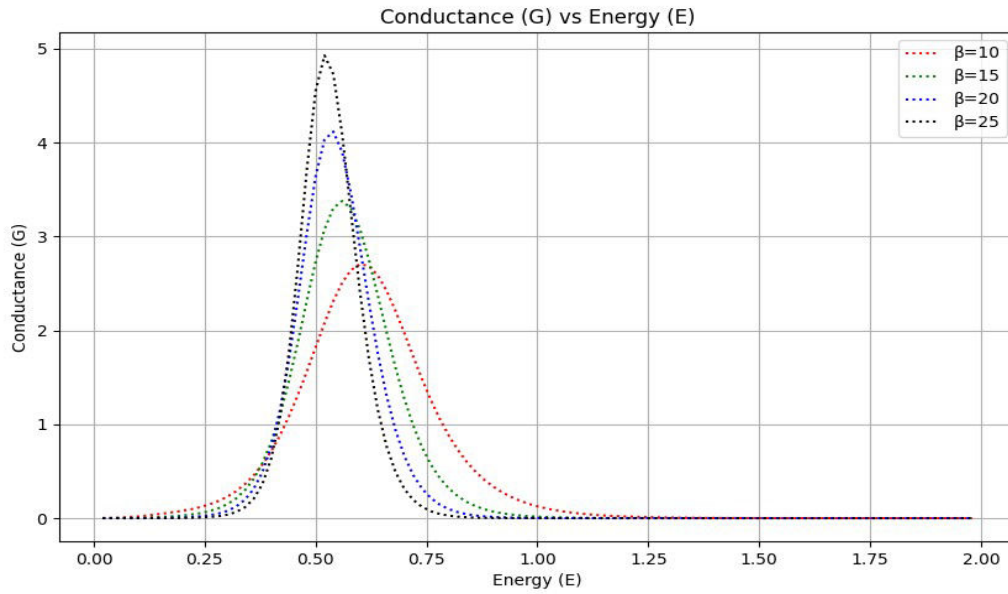


Figure 7: The conductance per energy of our model for the domain wall $J \gg D$. The value of the other parameters are: $\delta=0.1$, $\mu=0.5$ and $h=0.4$ where δ refers to the width of the domain wall and is equal to $\delta=D/J$, μ the chemical potential and h the value of the potential barrier.

We can observe that the conductance line in our model becomes sharper as the temperature decreases and approaches a type of δ function as $E \rightarrow \mu$ which is obvious since at zero temperature only the electrons at the Fermi energy contribute to the conductance.

The next graph (Figure 8) shows how the conductance behaves for different values of the chemical potential. For a smaller value of μ the conductance has a lower maximum value and as the chemical potential increases the maximum value of the conductance also increases. This is obvious since for larger values of the chemical potential the conducting electrons have a much larger probability to transmit through the potential barrier. After a certain point the transmission probability becomes almost saturated.

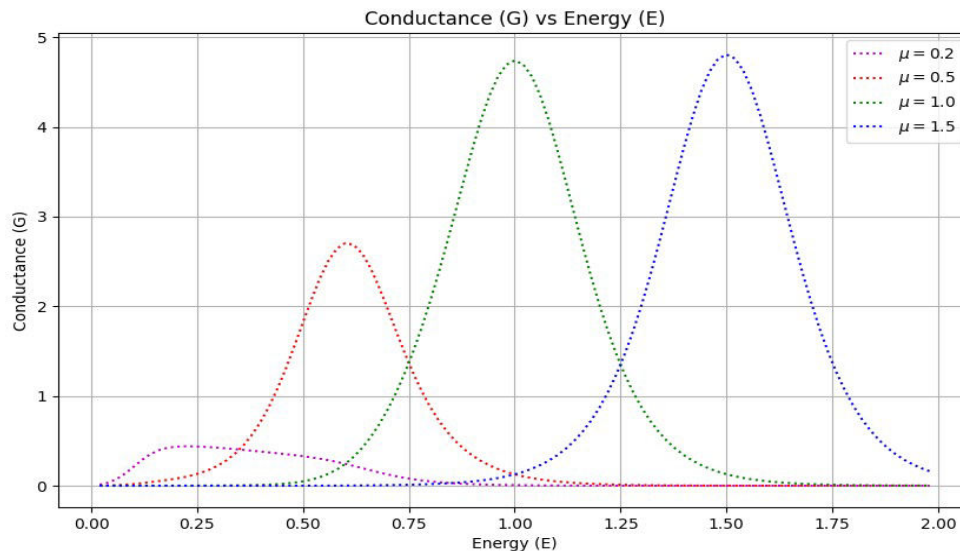


Figure 8: Conductance per energy for different values of μ . Also $\delta=0.1$, $\beta=10$, $h=0.4$.

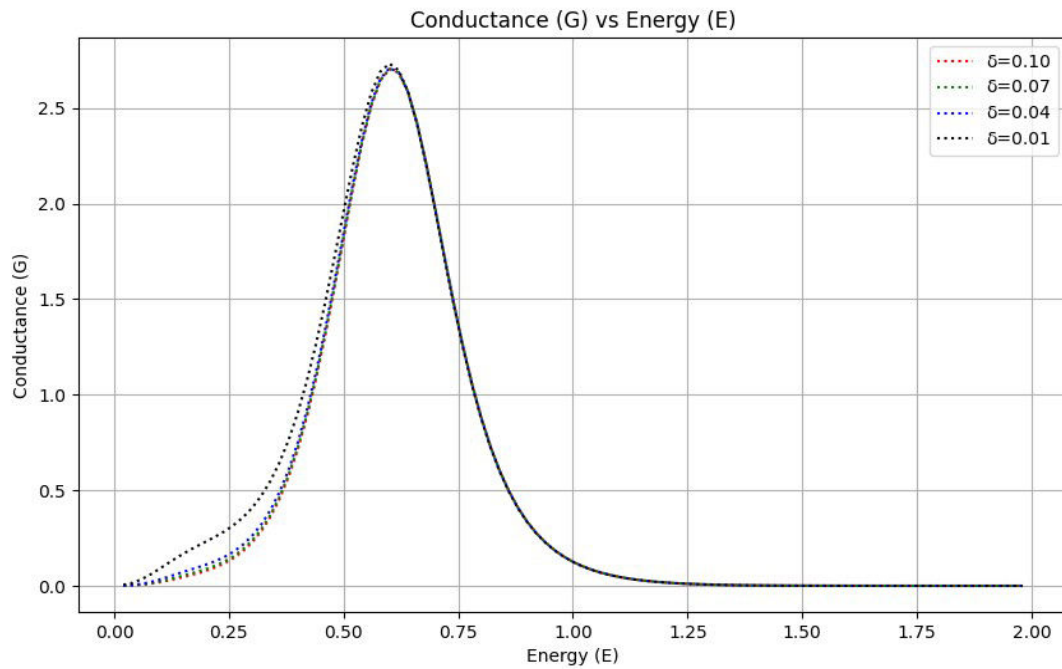


Figure 9: Conductance per energy for different widths of the domain wall. Also $\mu=0.5$, $\beta=10$ and $h=0.4$.

The first new data come when we try to examine the relationship between the conductance and the width of the domain wall (Figure 9). The surprising information we can extract is that the width does not affect at all the conductance for $E > \mu$ and there is a very small dependence for $E < \mu$.

It is also very interesting to see how the density of states is configured in this model (Figure 10). In the following graph we have plotted the density of states with respect to the electron energy for different values of the width of the domain wall. We can observe, similarly with the case of the conductance, that the width of the domain wall does not affect the system in an important way. However we can see that there is a slight deviation of the density of states curve when we alter the width for energy values that are smaller than the chemical potential.

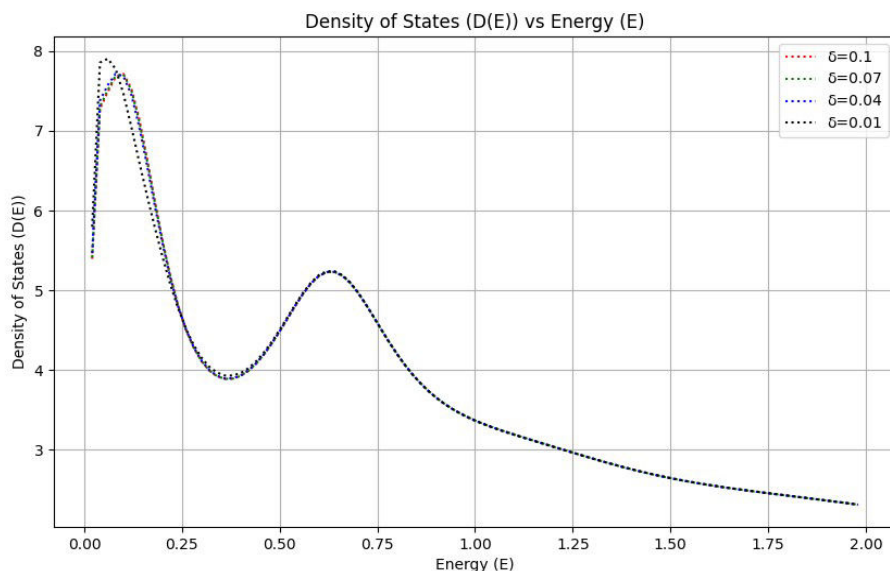


Figure 10: The density of states graph for each energy level and for different widths of the domain wall. Again $\mu=0.5$, $\beta=10$ and $h=0.4$.

For the domain wall D~J:

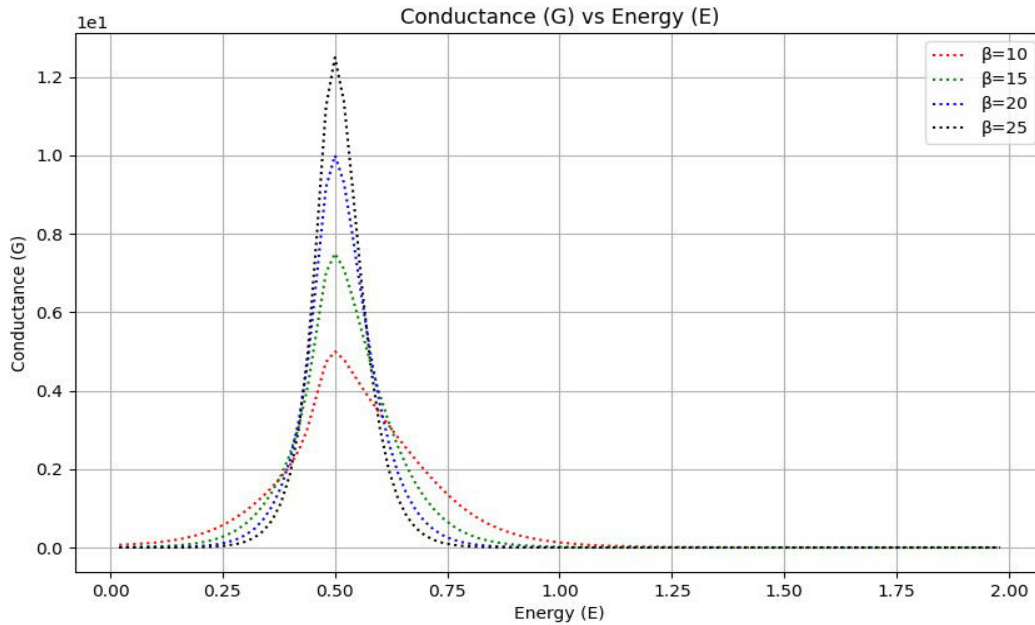


Figure 11: Conductance per energy for different temperatures. Also $\mu=0.5$, $\delta=1.0$ and $h=0.4$.

The diagram above features, as in the previous case, the dependence of the conductance from the electron energy for different temperatures. We can notice once again the expected behavior where the curve tends to a δ type function as the temperature decreases meaning that only the electrons in the Fermi level contribute to the conductance. However, to compare it with the previous structure of the domain wall, we can see that the curves are completely localized around the value of the chemical potential of the crystal even though all of the other parameters are the same. This means that the scattering matrix elements in eq. 3 are do not depend on the energy and only the partial derivative of the Fermi function determines the position of the peak of the line, which is at the value of the chemical potential.

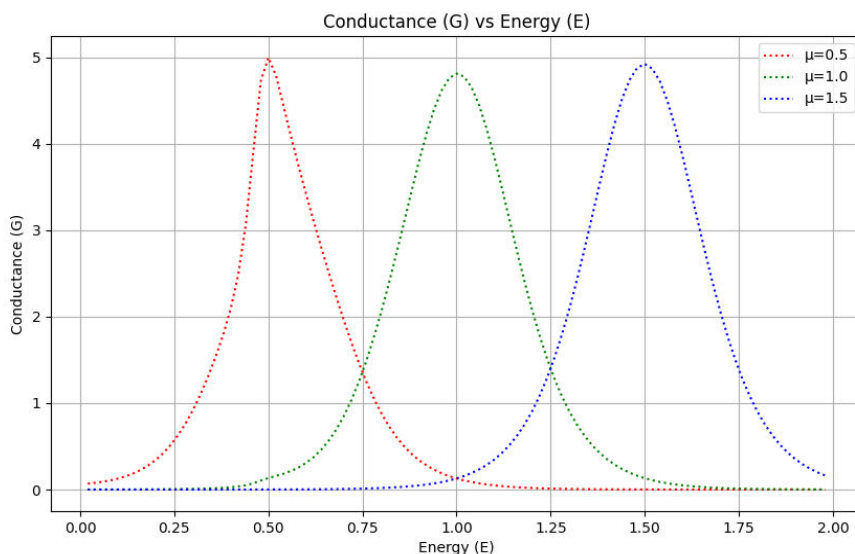


Figure 12: Conductance per energy for different values of the chemical potential. Also $\delta=1$, $\beta=10$, $h=0.4$.

We continue our investigation with the dependence of the conductance from the chemical potential (figure 12). Some very interesting results occur from it as we can see that the maximum value of the conductance remains the same as the chemical potential increases (we study the case where the chemical potential μ is greater than the potential barrier $h=0.4$). This means that the conductance gets saturated much faster than the case of the previous domain wall. Also the curves are localized around the value of μ (same as the previous figure) and we can see that the first curve is sharper than the other ones.

It is also notable that the conductance shows no dependence on the width of the domain wall.

Now for the last case we plotted the density of states of the system for this specific form of the domain wall. It is again invariant under the domain wall width alterations and seems to have a very different structure for the one that corresponds to the previous domain wall.

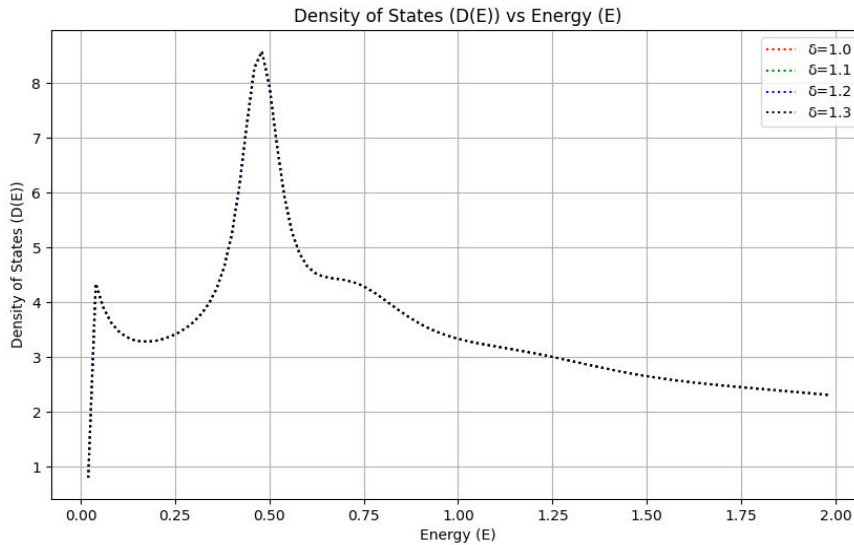


Figure 13: The density of states for the different energies. It is invariant from the width of the domain wall.

DISCUSSION

Our method was based on a double exchange (s-d) Hamiltonian approach along with the transfer matrix method in order to investigate the interaction between the electron and the domain walls. The primary goal was to analyze the conductance and the density of states of the system considering the transmission of the electrons through the domain walls as a scattering problem. Looking back to the graphical results of our model we can see that we get some very interesting output. The study of the electron-domain wall interaction is a very promising subject of study with many significant

applications. This project is part of a bigger effort to understand the dynamics and the final configuration of the domain walls when they interact with a fermionic gas.

REFERENCES

- [1] Biswas, D., & Kumar, V. (2014). Improved transfer matrix methods for calculating quantum transmission coefficient. *Physical Review. E, Statistical, Nonlinear and Soft Matter Physics*, 90(1). <https://doi.org/10.1103/physreve.90.013301>
- [2] Dashen, R., Ma, S., & Bernstein, H. J. (1969). S-Matrix Formulation of Statistical mechanics. *Physical Review*, 187(1), 345–370. <https://doi.org/10.1103/physrev.187.345>
- [3] Souma, S., & Suzuki, A. (2002). Local density of states and scattering matrix in quasi-one-dimensional systems. *Physical Review. B, Condensed Matter*, 65(11). <https://doi.org/10.1103/physrevb.65.115307>
- [4] Avishai, Y., & Band, Y. B. (1985). One-dimensional density of states and the phase of the transmission amplitude. *Physical Review. B, Condensed Matter*, 32(4), 2674–2676. <https://doi.org/10.1103/physrevb.32.2674>
- [5] Landauer–Büttiker formalism. (2011). In *IMPERIAL COLLEGE PRESS eBooks* (pp. 1–33). https://doi.org/10.1142/9781848168350_0001
- [6] Gasparian, V., Christen, T., & Buttiker, M. (1996). Partial densities of states, scattering matrices, and Green’s functions. *Physical Review. A, Atomic, Molecular, and Optical Physics/Physical Review, a, Atomic, Molecular, and Optical Physics*, 54(5), 4022–4031. <https://doi.org/10.1103/physreva.54.4022>
- [7] Stafford, C. A., Baeriswyl, D., & Bürki, J. (1997). Jellium Model of Metallic nanocoherence. *Physical Review Letters*, 79(15), 2863–2866. <https://doi.org/10.1103/physrevlett.79.2863>
- [8] Pianet, V., Urdampilleta, M., Colin, T., Clérac, R., & Coulon, C. (2017). Domain walls in single-chain magnets. *Physical Review. B./Physical Review. B*, 96(21). <https://doi.org/10.1103/physrevb.96.214429>
- [9] Yamanaka, M., & Nagaosa, N. (1996). Conductance through a Magnetic Domain Wall in Double Exchange System. *Journal of the Physical Society of Japan*, 65(9), 3088–3089. <https://doi.org/10.1143/jpsj.65.3088>
- [10] Department of Materials Science and Metallurgy - University of Cambridge. (n.d.-b). *Domain walls*. Creative Commons Attribution - NonCommercial-ShareAlike 4.0 International. <https://www.doitpoms.ac.uk/tlplib/ferromagnetic/walls.php>

- [11] <https://eepower.com/technical-articles/understanding-the-different-properties-of-diamagnetic-paramagnetic-and-ferromagnetic-materials/#>
- [12] Libretexts. (2021, May 1). 6.2: *b- the transfer matrix method*. Physics LibreTexts.https://phys.libretexts.org/Bookshelves/Quantum_Mechanics/Quantum_Mechanics_III_%28Chong%29/06%3A_Appendices/6.02%3A_B-The_Transfer_Matrix_Method